

Single cell mechanics: stress stiffening and kinematic hardening

Pablo Fernández* and Albrecht Ott†

Experimentalphysik I, Physikalisches Institut, Universität Bayreuth, D-95440 Bayreuth, Germany

(Dated: February 6, 2020)

Cell mechanical properties are fundamental to the organism but remain poorly understood. We report a comprehensive phenomenological framework for the nonlinear rheology of single fibroblast cells: a superposition of elastic stiffening and viscoplastic kinematic hardening. Our results show, that in spite of cell complexity its mechanical properties can be cast into simple, well-defined rules, which provide mechanical cell strength and robustness via control of crosslink slippage.

PACS numbers: 87.15.La, 87.16.Ka, 83.60.Df, 83.60.La

Intracellular transport, cell locomotion, resistance to external mechanical stress and other vital biomechanical functions of eukaryotic cells are governed by the cytoskeleton, an active biopolymer gel [1]. This gel is made of three types of biopolymers, actin, microtubules and intermediate filaments, crosslinked by a multitude of proteins with different properties in terms of connection angles, bond strengths and bond lifetimes. The actin cytoskeleton—the major force-sustaining structure in our experiments—is made of filaments of about micrometer length and presents a weak local structural order. The cytoskeleton also comprises molecular motors, proteins that move on actin or microtubule filaments driven by chemical energy. How the cytoskeleton in conjunction with biochemical regulatory circuits performs specific, active mechanical tasks is not understood. When cells attach to biological material they often biochemically recognize the binding partner. The cytoskeleton organizes accordingly and produces a mechanical response. Active cell responses such as contraction are well separated from passive rheological properties by their timescales [2]. Passive rheological cell properties have been studied with various techniques on subcellular and supercellular scale [3]. From the measurements with different techniques on different eukaryotic cell types a broad relaxation spectrum arises as a common feature of passive, linear cell rheology [3, 4]. However, the description of the non-linear regime remains elusive.

In the following we present microplate rheology experiments where individual cells are stretched between two plates (Fig. 1). The advantage of the setup is that the cells possess a well-controlled geometry and adhere via chosen biochemical linkers, which better define the cytoskeletal state. Quasi-differential cell deformations reveal an elastic stiffening response. The corresponding nonlinear elastic modulus depends on the cell prestress but is independent of cell length; it is described by a master curve including a transition from linear to nonlinear elasticity. Large deformations reveal a plastic regime with a (counterintuitive) linear force–length relation. Both relations simply superpose to generate the response to more complex deformations. The cell response reduces to the

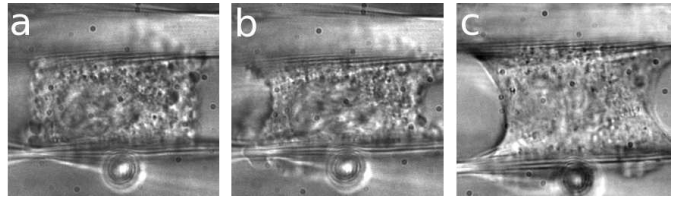


Figure 1: A fibroblast adhering between two microplates. **a:** Right after contact. **b:** After 20 min at 35°C the cell adopts a concave shape, a reproducible feature of strongly adhering fibroblasts. **c:** After a large stretch. Typical cell sizes are about 20 μm .

integral of the differential measurement when the plastic response is abolished by fixation. Hence, in spite of the complexity of the eukaryotic cell cytoskeleton and large cell heterogeneity, passive nonlinear cell rheology can be reduced to simple rules.

Experimental setup— We refer to Refs. [2, 5] for details. A 3T3 fibroblast [6] adheres between two fibronectin-coated glass microplates. One of them is flexible: its deflection gives the perpendicular force F acting on the cell. This plate is translated by a piezoelectric actuator controlled by a personal computer. The computer calculates force F and cell length ℓ , and adjusts the piezo position via a proportional feedback loop to impose a given experimental protocol. All results described here are fully reproducible for fibroblasts which adhere sufficiently strongly to sustain pulling forces of 100 nN for several hours, which means about 30% of the cells in culture.

Loading and unloading at constant rate— We stretch the cell by 100% at a constant rate $\dot{\ell}$ while measuring the force F (Fig. 2a). Then the cell length ℓ is held constant for a few minutes; we observe stress relaxation. The cell is unloaded back to the initial length with the opposite rate, $-\dot{\ell}$, and again held at constant length. The procedure is repeated with different rates $\dot{\ell}$ between 3 nm/s and 10 $\mu\text{m/s}$. At the beginning of the ramp, the slope $dF/d\ell$ steadily decreases, reaching a constant value at an elongation $\sim 10\%$ (Fig. 2b). Beyond 10% and up to 100% stretch, the $F(\ell)$ relation is in most cases linear. Within the explored loading rates, the slope $dF/d\ell$ never increases during a ramp. After the ramp, the force F relaxes to a steady non-zero value \mathfrak{F} which does not evolve faster than ~ 1 nN/s. The hysteresis loop becomes wider with increasing stretch rate $\dot{\ell}$. The asymptotic slope $dF/d\ell$ and the equilibrium force \mathfrak{F} are independent of the loading rate in the explored range of 3 decades.

*Present address: Lehrstuhl für Biophysik E22, Technische Universität München, James Franck Straße, D-85748 Garching, Germany

†Present address: Experimentalphysik, Universität des Saarlandes, D-66041 Saarbrücken, Germany

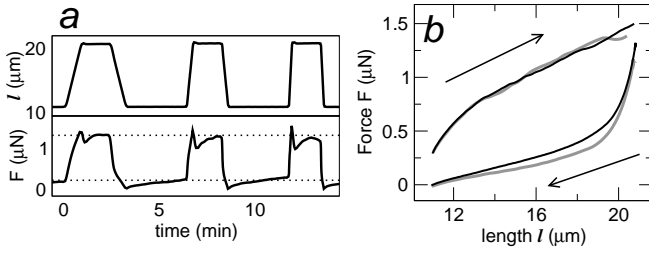


Figure 2: Loading and unloading at constant rate $\dot{\ell}$. **a**: Force F and length ℓ as a function of time. After each ramp, F relaxes and stabilizes at a nonzero value \mathfrak{F} (dotted line). **b**: F as a function of ℓ during loading and unloading. Black curve: $\dot{\ell} = 0.5 \mu\text{m/s}$. Grey curve: $\dot{\ell} = 5 \mu\text{m/s}$.

Small amplitude stiffening, large amplitude linearity— To explore small and large deformation amplitudes simultaneously we perform a loading ramp with superimposed harmonic oscillations, imposing $\ell(t) = vt + \Delta_\ell \sin(\omega t)$. Fig. 3 shows a typical experiment. The response to small oscillations indeed stiffens with increasing stress. Yet, the averages over an oscillation period of the force $\langle F \rangle$ and length $\langle \ell \rangle$ are linearly related as inferred from the position of the loops. Therefore, we observe both responses *simultaneously*: stiffening at small amplitudes, as reported earlier [5], and linearity at large amplitudes.

Small amplitude reversibility, large amplitude irreversibility— We study the amplitude dependence, at a constant deformation rate $|\dot{\ell}|$. An essential feature of the measurement-protocol are the turning points separated at various distances in order to study the reversibility of the response (Fig. 4a). Similar procedures can be found in plasticity textbooks [7]. The reversibility of the response upon a change of direction is determined by the distance to the previous turning point. Where turning points are separated by less than 10% stretch, the response is reversible (elastic). More than 10% stretch beyond a turning point, the response becomes irreversible (plastic): the $F(\ell)$ curve does not retrace its path upon direction reversal (Fig. 4b). In this plastic regime the $F(\ell)$ relation is approximately linear. The consequence of its nonzero slope is a translation of the elastic region by the plastic deformation, a behavior known in plasticity as linear kinematic (or directional) hardening

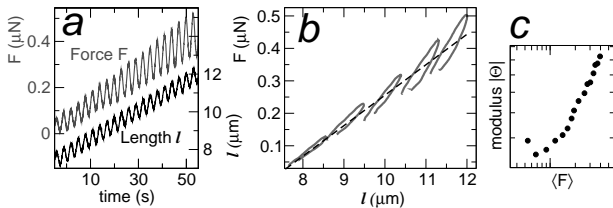


Figure 3: Small amplitude stiffening, large amplitude linearity. **a**: F and ℓ as a function of time. **b**: F as a function of ℓ . For clarity, only a few loops are shown. The dashed line highlights the linear relation between the average values. **c**: Differential modulus $|\Theta|$ as a function of average force $\langle F \rangle$ for the data shown in b. The response to the small oscillations shows stiffening, following the master-relation reported in [5].

[7, 8, 9, 10]. Alternatively, the plastic contraction under *pulling* tension between X and G in Fig. 4b is a strong Bauschinger effect [7, 11].

Combining kinematic hardening with a nonlinear elastic response rationalizes our results (Fig. 4e). Small deformations remain inside the elastic region, where stress stiffening is observed (the tilting of the loops in Fig. 3). Large deformations become plastic as they reach the rim of the elastic region. As the plastic deformation proceeds further along the edge, a linear $F(\ell)$ relation is observed (as in Fig. 2). Upon a change of direction the elastic region is immediately reentered (as in Fig. 4b, turning points D, F, G, I).

Large amplitude stiffening after glutaraldehyde fixation— We add glutaraldehyde 0.1% with the aim of preventing slippage of cytoskeletal connections. Glutaraldehyde, routinely used as a fixing agent for microscopy, is known to preserve the ultrastructure of the cytoskeleton [12]. Loading at constant rate (Fig. 5a) reveals a positive curvature $d^2F/d\ell^2$ (Fig. 5b). The numerical derivative of the $F(\ell)$ relation obtained from fixed (hence dead) cells is the same as the differential master-relation obtained on *living* fibroblasts (Fig. 5c, from Ref. [5]). The $F(\ell)$ relation after fixation closely resembles the exponential stress-stretch relations known from

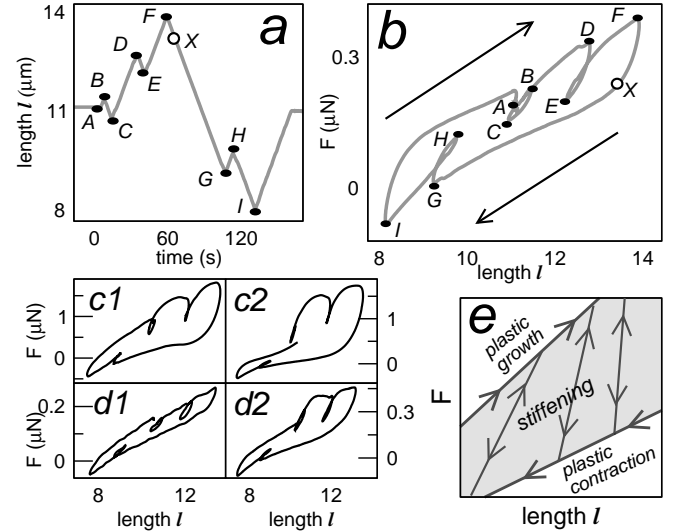


Figure 4: Elastoplastic behavior. **a**: Imposed length ℓ as a function of time. **b**: F as a function of ℓ for a given cell. Reversible (elastic) behavior upon direction reversal is observed only close to a previous turning point, as in C, E, H. The response becomes irreversible (plastic) after a steady large deformation: at the turning points D, F, G, I, the $F(\ell)$ curve does not retrace its previous path. Between F and I the experiment is equivalent to C–F, but in the unloading direction. The response is seen to be equivalent, showing the sense of deformation to be irrelevant. **c1**: Another cell, probed at a rate $\dot{\ell} = 0.1 \mu\text{m/s}$. **c2**: Same cell as c1 but at $\dot{\ell} = 1 \mu\text{m/s}$. **d1**: Another cell, $0.1 \mu\text{m/s}$. **d2**: Same cell as d1, $1 \mu\text{m/s}$. **e**: Protocol-independent idealization of the response. The arrows indicate the possible direction of the deformation. The shaded area is the elastic (reversible) region; plastic (irreversible) deformation takes place along its edge. Stress stiffening tilts the paths inside the elastic region; kinematic hardening is the tilt of the elastic region itself.

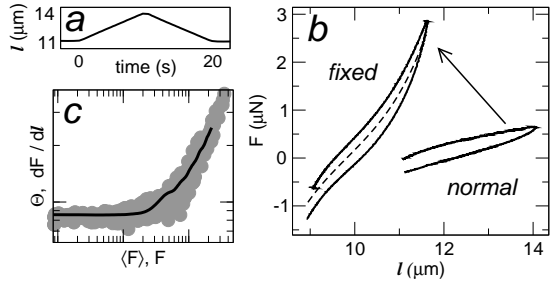


Figure 5: **a**: Imposed length ℓ as a function of time. A single loading cycle with amplitude 30% is performed. **b**: Force F as a function of length ℓ . “Normal”: before adding glutaraldehyde. “Fixed”: in presence of glutaraldehyde 0.1%. The dotted line is a fit to Eq.2. **c**: The derivative $dF/d\ell$ of the “fixed” curve (black line) plotted against the differential master-relation (gray dots, as discussed in Ref.[5]).

whole tissues [13, 14]. For incompressible materials under uniaxial extension, the hyperelastic strain energy proposed by Fung [13] gives Eq. 2 below.

Rate dependence— In the plastic flow regime the width of the hysteresis loops increases with increasing stretch rate (Fig. 6a). To characterize this rate-dependence, we define the overstress ΔF as the extent of force relaxation after unloading (Fig. 6a). The overstress ΔF behaves as $\sim \log(d\ell/dt)$, approaching zero at a non-zero pulling speed of about 10 nm/s (see Fig.6 b).

Viscoplasticity— We now propose a minimal constitutive relation for fibroblasts under uniaxial extension. First we decompose the measurable cell length ℓ into a plastic rest length \mathfrak{L} and elastic stretch ratio λ ,

$$\ell = \lambda \mathfrak{L}. \quad (1)$$

The force is a function solely of the elastic strain,

$$F \propto (\lambda - 1)e^{\gamma(\lambda^2 + 2/\lambda - 3)}, \quad (2)$$

where for concreteness we use exponential elasticity [13], according to Fig. 5b, c. As a flow rule relating the plastic strain rate $\dot{\mathfrak{L}}$ to the force F , we propose an exponential function of the overstress $F - \mathfrak{F}$, according to Fig. 6b:

$$\dot{\mathfrak{L}} \propto \text{sgn}(F - \mathfrak{F}) e^{|F - \mathfrak{F}|/\mathcal{D}}. \quad (3)$$

The equilibrium force \mathfrak{F} is the essential internal variable to describe kinematic hardening [7, 8, 10]. The force scale is defined by another internal variable, the drag force \mathcal{D} . To describe the stiffening response of both moduli [5], the drag \mathcal{D} must be proportional to the nonlinear modulus, $\partial F/\partial \lambda|_{\mathfrak{L}}$. Finally, Eq.4 gives linear kinematic hardening:

$$\dot{\mathfrak{F}} \propto \dot{\mathfrak{L}}. \quad (4)$$

This is a phenomenological description along the lines of modern viscoplasticity [7, 10, 11], without explicit history dependencies. As Fig. 7 shows, it captures the essential features of our experiments. At small amplitudes, $|F - \mathfrak{F}| \ll \mathcal{D}$, the deformation is essentially elastic: $\dot{\ell} \sim \dot{\lambda}$. At large amplitudes

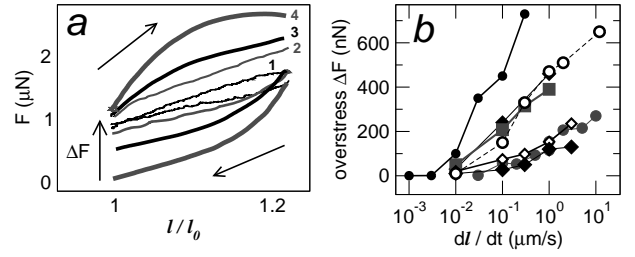


Figure 6: Loading and unloading for several rates $\dot{\ell}$. **a**: F as a function of ℓ/ℓ_0 for a given cell, where ℓ_0 is the initial length. Rates are: 1) 10 nm/s, 2) 30 nm/s, 3) 0.1 $\mu\text{m/s}$, 4) 1 $\mu\text{m/s}$. The overstress ΔF is defined as the extent of relaxation after unloading. **b**: Rate $\dot{\ell}$ as a function of ΔF for 7 different cells.

the overstress $|F - \mathfrak{F}|$ approaches the drag stress \mathcal{D} and the deformation becomes increasingly plastic: $\dot{\ell} \sim \dot{\mathfrak{L}} \propto \dot{\mathfrak{F}} \sim \dot{F}$.

Microscopic mechanisms— Our glutaraldehyde fixation experiments show that stress stiffening in fibroblasts [5] is due to the nonlinear elasticity of the cytoskeleton, unrelated to biological signalling or restructuring processes. In agreement, very similar stiffening is known from biopolymer networks [15]. To date the precise microscopic mechanism remains unclear; stretching [15, 16] and bending [5, 17] of single filaments as well as alignment of filaments along the stretch direction [18] have been proposed.

The energy to reach the linear plastic regime in loading experiments (from Fig. 2) is $\sim 1\mu\text{N}\mu\text{m} \simeq 2.5 \cdot 10^8 k_B T$. During stretch, first elastic elements must be loaded, until they dissipate the stored energy upon bond rupture. Cells which adhere to a substrate increase their dissipation through elasticity by 100 times compared to bond adhesion energies [19]. Taking the bond energy as $10 k_B T$ [20] and the actin cytoskeleton meshsize as 100 nm, a substantial fraction of about 0.1–1 of the actin cytoskeletal bonds must be ruptured to reach stationary flow. However, in order to observe the stress stiffening master relation (Fig. 3) ubiquitously during plastic deformation, the actin gel must remain above percolation threshold—even during our most rapid stretching experiments. For a gel with one bond relaxation time viscous drag is expected to decrease with speed v as $1/v$ when bonds fail to reconnect above a certain deformation rate [21], which would give a

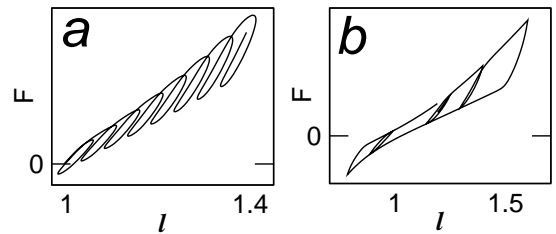


Figure 7: Eqs. 1–4 for deformation protocols like those in Fig. 3 and Fig. 4, taking $\gamma = 5$ and $\mathcal{D} = 0.01 \partial F/\partial \lambda|_{\mathfrak{L}}$. This protocol-independent phenomenological description captures small-amplitude elastic stiffening and large-amplitude viscoplastic linearity.

rate-independent overstress. We observe an exponential rate-overstress dependence. In general, dissociation rates depend on the force per bond f as $\sim e^{f/f_0}$, with a force scale $f_0 \sim 10$ pN [22, 23]. In agreement, in fibroblasts the drag \mathcal{D} is about 100 nN, corresponding to 1–10 pN per filament.

The combination of a sharply rising rate-overstress dependence and kinematic hardening must prevent cell breakage in our large deformation experiments. A cell portion under increased stress will readily flow and increase its equilibrium stress to reach a stable situation. This avoids non-affine situations of the actin gel. In uniaxial elongation, rather than break at a given spot the cell must prolong homogeneously along its length in order to accommodate the plastic deformation. This homogeneous deformation may even be behind the robust linearity of the kinematic hardening response, since integration of a constant magnitude along the cell length would naturally give a linear length dependence. However, identification of the precise molecular mechanisms behind this unusual behavior in a soft system is a task for the future. At least, one can rule out an interpretation in terms of a Hookean spring element (in form of intermediate filaments, for example) in parallel with a nonlinear, viscoelastic actin gel obeying the master-relation [24]. Hardening and stiffening must originate in one and the same mechanical element. This scenario reminds of composite alloys [11] and granular materials [9], where kinematic hardening arises as the plastic flow induces alterations of directional nature to the microstructure.

Linear responses to large stretch have been observed before in single cells [25], cell populated gels [26] and cell monolayers [27]. Here we show that this linearity must be understood

as a plastic hardening response. Living cells can neither be purely elastic objects, nor possess a yield stress within the biological “working range”. Kinematic hardening viscoplasticity appears as an elegant way to match these conditions. Furthermore, by actively controlling the extent of plastic flow the cell can deploy the elastic stiffening response to a chosen extent. In our glutaraldehyde-fixation experiment an order of magnitude increase in the overall stiffness is obtained, presumably by simply switching from slipping to sticking contacts. As a final remark, the plastic stretch rate where the cell flows without friction is of the order of 10^{-3}s^{-1} , which compares well to active processes [1, 3]. Thus, active biological plastic phenomena take place at zero overstress, at the rate given by spontaneous bond dissociation. This may explain the timescale separation of active and passive responses [2].

Summarizing, we have shown that cell mechanical properties in uniaxial stretching experiments can be thoroughly described by the superposition of two simple relations: exponential elasticity, and viscoplasticity with linear kinematic hardening. Given the cytoskeletal complexity, this is unexpected. A complete picture of passive cell rheology spanning from molecular details to a simple phenomenological description and straightforward theoretical concepts seems in close reach.

We are very grateful to P. A. Pullarkat for his invaluable advice and support. P. F. sincerely thanks K. Kroy for revealing discussions as well as financial support. Thanks are also due to N. Aksel, R. Everaers, F. Jülicher and S. Kumar for their criticism, which inspired much of this work. This work has been funded by the Universität Bayreuth.

-
- [1] D. Bray, *Cell Movements : from molecules to motility* (Garland Publishing, Inc., New York, 2001), 2nd ed.
- [2] O. Thoumine and A. Ott, *J. Cell. Sci.* **110**, 2109 (1997).
- [3] P. A. Pullarkat, P. A. Fernández, and A. Ott, *Phys. Rep.* (doi: 10.1016/j.physrep.2007.03.002) (2007).
- [4] B. Fabry, G. N. Maksym, J. P. Butler, M. Glogauer, D. Navajas, and J. J. Fredberg, *Phys. Rev. Lett.* **87**, 148102 (2001).
- [5] P. Fernández, P. A. Pullarkat, and A. Ott, *Biophys. J.* **90**, 3796 (2006).
- [6] G. J. Todaro and H. Green, *J. Cell. Biol.* **17**, 299 (1963).
- [7] J. Lubliner, *Plasticity theory* (Macmillan Publishing Company, New York, 1990), 1st ed.
- [8] W. Prager and H. Geiringer, *Ergebnisse der exakten Naturwissenschaften* **13** (1934).
- [9] S. Nemat-Nasser, *Plasticity: A Treatise on Finite Deformation of Heterogeneous Inelastic Materials* (Cambridge University Press, 2004).
- [10] E. Krempl, in *Unified constitutive laws of plastic deformation*, edited by A. S. Krausz and K. Krausz (Academic Press, San Diego, 1996), pp. 281–318.
- [11] U. F. Kocks, in *Unified constitutive equations for creep and plasticity*, edited by A. Miller (Elsevier applied sciences, Essex, 1987), pp. 1–88.
- [12] J. V. Small, K. Rottner, P. Hahne, and K. I. Anderson, *Microsc. Res. Tech.* **47**, 3 (1999).
- [13] Y. C. Fung, *Biomechanics: Mechanical properties of living tissues* (Springer Verlag, New York, 1993).
- [14] Exponential elasticity can also be revealed by microrheological techniques. B. Fabry, personal communication.
- [15] C. Storm, J. J. Pastore, F. C. MacKintosh, T. C. Lubensky, and P. A. Janmey, *Nature* **435**, 191 (2005).
- [16] E. Kuhl, K. Garikipati, E. M. Arruda, and K. Grosh, *J. Mech. Phys. Solids* **53**, 1552 (2005).
- [17] A. Kabla and L. Mahadevan, *J. R. Soc. Interface* **4**, 99 (2007).
- [18] P. R. Onck, T. Koeman, T. van Dillen, and E. van der Giessen, *Phys. Rev. Lett.* **95**, 178102 (2005).
- [19] E. Décavé, D. Garrivier, Y. Bréchet, F. Bruckert, and B. Fourcade, *Phys. Rev. Lett.* **89**, 108101 (2002).
- [20] A. Mogilner and G. Oster, *Biophys. J.* **71**, 3030 (1996).
- [21] F. Gerbal, V. Noireaux, C. Sykes, F. Jülicher, P. Chaikin, A. Ott, J. Prost, R. M. Golsteyn, E. Friederich, D. Louvard, et al., *Pramana - J. Phys.* **53**, 155 (1999).
- [22] G. I. Bell, *Science* **200**, 618 (1978).
- [23] D. A. Simson, M. Strigl, M. Hohenadl, and R. Merkel, *Phys. Rev. Lett.* **83**, 652 (1999).
- [24] It would require a coupling between the two elements.
- [25] S. Yang and T. Saif, *Exp. Cell Res.* **305**, 42 (2005).
- [26] T. Wakatsuki, M. S. Kolodney, G. I. Zahalak, and E. L. Elson, *Biophys. J.* **79**, 2353 (2000).
- [27] P. Fernández, L. Heymann, A. Ott, N. Aksel, and P. A. Pullarkat, submitted (2007).